Environmental Science Nano

PAPER

View Article Online
View Journal | View Issue

Check for updates

Cite this: *Environ. Sci.: Nano*, 2025, **12**, 4935

Quantitative evaluation of true-to-life nanoplastics using UV-visible spectroscopy and comparative analytical techniques

Serena Ducoli,[ab] Géraldine Dumont,[cd] Milica Velimirovic,[c] Dora Mehn,[e] Mariacristina Cocca,[f] Laura E. Depero[ab] and Stefania Federici[*ab]

Received 21st May 2025,
Accepted 22nd September 2025

DOI: 10.1039/d5en00502g

rsc.li/es-nano

The growing concern over microplastic pollution has led to increased focus on environmental nanoplastics, which are smaller, more dynamic, and present unique challenges in both quantification and risk assessment. Nanoplastics exhibit high variability in size, shape, chemical composition, and surface chemistry, complicating their detection and quantification through conventional analytical techniques developed for nanomaterial analysis. One of the key challenges in nanoplastic research is the lack of realistic, environmentally relevant test materials that accurately mimic the characteristics of nanoplastics found in natural environments. In this study, we generated polystyrene-based nanoplastics from fragmented plastic items and use them to produce controlled test materials for evaluating and comparing analytical techniques under well-defined conditions. Specifically, we investigated the potential of microvolume UV-visible (UV-vis) spectroscopy as a practical and non-destructive technique for the quantification in stock suspensions, aiming to expand the analytical toolkit for environmental nanoplastic research. UV-vis spectroscopy was compared with established mass-based techniques, pyrolysis gas chromatography-mass spectrometry and thermogravimetric analysis, as well as nanoparticle tracking analysis, a number-based method. The comparative analysis demonstrated that UV-vis spectroscopy provides a rapid, accessible, and effective mean of quantifying nanoplastics, especially when sample volumes are limited. Despite some underestimation of nanoplastic concentrations relative to mass-based techniques, UV-vis measurement results were consistent in terms of order of magnitude, showing reliable trends across different methods. This study underscores the potential of UV-vis spectroscopy as a valuable tool for quantifying realistic nanoplastic test materials and supporting the development of future applications in environmental nanoplastic research.

Environmental significance

The detection and quantification of nanoplastics in environmental samples remain a major challenge in assessing their ecological and human health risks. This study addresses a critical gap by evaluating UV-visible spectroscopy as a rapid and accessible method for quantifying nanoplastics that were intentionally generated under controlled conditions to mimic environmentally relevant materials. The key finding is that UV-vis provides reliable quantification for complex, environmentally relevant stock suspensions of test nanoplastics when benchmarked against established mass- and number-based techniques. These results can be generalized to support method development for broader environmental monitoring efforts. By advancing analytical capabilities, this work contributes to our understanding of nanoplastic behavior in the environment and informs future risk assessments, regulatory efforts, and mitigation strategies aimed at protecting ecosystems and human health.

1. Introduction

Environmental micro- and nanoplastic pollution affects nowadays every environmental compartment, threatening the delicate balance of many ecosystems. The degradation of plastics requires hundreds of years and, due to physical processes like erosion or fragmentation, vast quantities of particles have been accumulating in all the environmental compartments.[1] In recent years, research has focused on

[a] *Department of Mechanical and Industrial Engineering, University of Brescia, Brescia, Italy. E-mail: stefania.federici@unibs.it*
[b] *National Interuniversity Consortium of Materials Science and Technology (INSTM), Florence, Italy*
[c] *Flemish Institute for Technological Research (VITO), 2400 Mol, Belgium*
[d] *Organic and Biological Analytical Chemistry Group, MolSys Research unit, University of Liège, 4000 Liège, Belgium*
[e] *European Commission, Joint Research Centre (JRC), Ispra, Italy*
[f] *Institute of Polymers, Composites and Biomaterials – National Research Council of Italy, Pozzuoli, Italy*

identifying these particles in the environment,[2] evaluating risks for organisms,[3] assessing bioaccumulation,[4] and modelling environmental dispersion.[5] Despite this growing body of research, significant knowledge gaps remain that may affect the relevance and the reliability of existing data, particularly regarding the toxicological and environmental effects of the finest fraction represented by nanoplastics (NPs).[6] NPs are generally defined as plastic particles with at least one dimension below 1 μm; however, the definition is still under debate, with some authors setting the size range between 1 and 1000 nm,[7,8] while others propose lower or higher boundaries, such as an upper size limit of 100 nm or no clear lower size threshold.[9] The inherent characteristics of NPs, including the small size, the high surface/volume ratio, the variable and unpredictable chemical composition, and size/shape variability, distinguish NPs from both microplastics and synthetic nanomaterials and hamper the translation of conventional analytical procedures for their characterization and quantification.[10] The result is a lack of knowledge and consensus on NP abundance in the environment, which prevents the evaluation of the threats associated with NP exposure. This information is also essential for carrying out toxicological and ecotoxicological assays to determine the harmful effect of NPs on human health and ecosystems. Moreover, understanding these characteristics is crucial for risk assessment, as they influence NPs' bioavailability, persistence, and interactions with biological and environmental systems, ultimately shaping exposure scenarios and hazard evaluations.[11,12]

So far, only a few studies have succeeded in isolating NPs from the environment,[13,14] a task that still remains a scientific challenge in terms of instrumentation limits and complexity of the environmental matrices, which both contribute to the difficulties of NP isolation, detection, and quantification.[15]

To overcome these limitations, studies are moving towards the generation and use of realistic test NPs, sometimes referred to in the literature as true-to-life NPs, made following top-down fragmentation approaches. These efforts aim to assess and refine analytical protocols, build trustworthy databases, and move a step closer to addressing the gap in the nanotoxicology of environmental samples, while also striving to harmonize methods and contribute to the development of reference materials, ensuring consistency and reliability in NP characterization across studies.[16–18]

Nevertheless, the analysis, and in particular the quantification, of NPs remains a significant challenge. This also applies to test materials and candidate reference materials, which often exhibit a high degree of variability in size, shape, surface chemistry, and aggregation behavior. These critical features complicate standardization efforts and highlight the need for robust, reproducible analytical approaches tailored to the complex nature of NPs, even in controlled laboratory settings.[19] This complexity affects the application of common nanoparticle analytical techniques based on light scattering and Brownian motion, such as dynamic light scattering and nanoparticle tracking analysis. While these methods offer valuable insights into size distribution and concentration in suspension, their effectiveness can be limited when dealing with highly polydisperse or irregular shaped NPs, necessitating complementary approaches for accurate characterization.[20] Other emerging techniques, including asymmetrical flow field-flow fractionation (AF4) and single-particle inductively coupled plasma mass spectrometry (SP-ICP-MS), have shown promise for size-resolved separation and elemental composition analysis of NPs, but they remain limited by high instrumentation costs, complex sample preparation, and sensitivity to environmental matrices.[21,22] The use of thermo-analytical techniques to identify and quantify NPs has recently been increasingly reported in the literature.[23,24] These techniques present the advantage of overcoming the size limitation issue encountered by other techniques, including infrared spectroscopy for instance.[25] On the other hand, thermo-analytical techniques do not provide any information concerning the shape, size or color, and their destructive principle prevents further analysis of the same sample.[25] Furthermore, the limited yield of NPs produced by current fragmentation techniques restricts the routine application of some traditional quantification methods, such as gravimetric analysis or mass-based techniques. These methods often require sample quantities in the scale range of μg or even the entire sample for analysis, making them impractical in cases when only small amounts of NPs are available. As a consequence, the sample used for initial characterization cannot be subdivided for further investigations, preventing a comprehensive characterization of the original sample across different techniques. This consideration can be extended to environmental NP samples, since the limited available data suggest a very low environmental NP concentration.[26,27]

In this study, we investigated the potential of UV-visible (UV-vis) spectroscopy as a practical, fast, and accessible technique for the quantification of test true-to-life NPs generated under controlled laboratory conditions as stock suspensions. In particular, UV-vis spectroscopy was used due to its widespread availability, rapid analysis time, and non-destructive nature. In detail, a microvolume UV-vis spectrophotometer was used offering key advantages, including its low sample demand system that allows for the measurement of scarce samples and enables sample recovery for subsequent analyses. These features make it particularly valuable in NP research, where sample conservation is often critical. To assess the reliability of this approach, we compared UV-vis measurement results with those obtained from established quantification methods, including mass-based techniques, namely pyrolysis gas chromatography-mass spectrometry (Py-GC-MS) and thermogravimetric analysis (TGA), and a number-based technique, nanoparticle tracking analysis (NTA). This comparative evaluation provided valuable insights into the robustness and complementarity of the established analytical methods, Py-GC-MS, TGA, and NTA, thereby reinforcing their role in the evolving field of NP analysis. This also highlights the value of using these methods in a multitechnique validation approach, ensuring a more comprehensive and reliable characterization of NPs.[19] At the same time, this allowed us to critically assess the strengths and

limitations of UV-vis spectroscopy, highlighting its potential as a rapid, accessible, and non-destructive tool for the quantification of true-to-life NPs produced under controlled laboratory conditions. Given the challenges posed by the variability of test materials, this study contributes to the ongoing efforts to harmonize NP characterization, providing a step toward more consistent and reproducible quantification protocols.

2. Materials and methods

2.1. Materials

White plastic disposable objects, with their polymeric content identified as polystyrene (PS), were selected to produce realistic test NPs (*viz.* true-to-life nanoplastics) by means of mechanical fragmentation. Polystyrene commercial nanobeads of 100 nm, 300 nm, 600 nm, 800 nm, and 1100 nm diameter (aqueous suspensions 10% w/v) were purchased from Merck Life Science S.r.l. (Milan, Italy). It is important to note that the fragmented NPs used in this study were obtained exclusively from white, unpigmented polystyrene materials. Colored or heavily pigmented plastics were not included. This choice was intentional to avoid potential interference from pigments in the UV-visible extinction spectra, which could obscure or alter the polymer absorbance signal and affect quantification accuracy. Since pigmented plastics are known to exhibit strong, broad absorption in the UV-visible range, further investigations will be required to assess the applicability of this UV-vis technique to NPs derived from colored or pigmented plastic waste.

2.2. Nanoplastic preparation

Selected PS objects were mechanically fragmented using an ultracentrifugal mill (ZM 200, Retsch GmbH, Haan, Germany) operating under cryogenic conditions to obtain a micrometric powder, as described in a previous study.[28] Polystyrene nanoplastics (PS NPs) were separated from the microplastics by suspending the PS powder in MilliQ water (Millipore Co., Bedford, USA, MA) in the ratio 0.1 g of PS powder : 30 mL of MilliQ water and following the protocol of sequential centrifugations previously developed.[28] The final pellets of PS NPs were resuspended in an appropriate volume of MilliQ water for subsequent analysis and quantification. Due to the specific requirements of each analytical technique, the volume of sample used for each measurement was not uniform across methods. For instance, TGA required the entire available sample to reach the instrument's limit of detection, while for NTA, only a defined aliquot could be injected per measurement. Py-GC-MS, on the other hand, required as little as 5–10 μL. These differences reflect the operational constraints of each instrument. However, in order to allow direct comparison between techniques, all results were normalized and reported with reference to the total processed sample volume.

2.3. Microvolume UV-vis spectroscopy

PS commercial nanobeads of different sizes (100 nm, 300 nm, 600 nm, 800 nm, and 1100 nm) were tested for their extinction spectra in the UV-vis region. For each size of PS nanobeads, at least six suspensions at known concentrations, from 5 μg mL^{-1} to 100 μg mL^{-1}, were prepared in Milli-Q water (Millipore Co., Bedford, USA, MA). Spectra were acquired using a NanoDrop One^{C} Microvolume UV-vis Spectrophotometer (Thermo Scientific™, Waltham, USA, MA) in the range 190–840 nm, directly spotting a droplet of 2 μL of each suspension onto the optical measurement surface. For microvolume measurements, the software selects the optimal pathlength (between 1.0 mm and 0.03 mm) based on sample absorbance at the analysis wavelength. Displayed spectra and absorbance values are normalized to a 10 mm pathlength equivalent. For each concentration, 3–5 replicate measurements were performed. The maximum of the extinction spectrum was calculated as the average of the replicates, and the corresponding standard deviation and coefficient of variation (CV%) were determined. The CV% was consistently below 3–4%, confirming high repeatability. Calibration curves were constructed by plotting the averaged extinction maxima against the known concentrations for each nanobead size. The calibration curve for 100 nm PS nanobeads showed excellent linearity (R^2 = 0.9994). To assess the sensitivity of the UV-visible spectroscopic method, the limit of detection (LOD) and limit of quantification (LOQ) were calculated following the IUPAC approach,[29] using the standard formulas: LOD = 3.3 × (σ/S) and LOQ = 10 × (σ/S), where σ is the standard deviation of the absorbance values measured at the lowest tested concentration (5 μg ml^{-1}), and S is the slope of the linear calibration curve. For 100 nm test nanobeads, the LOD and LOQ were calculated as: LOD = 0.818 μg ml^{-1} and LOQ = 2.48 μg ml^{-1}. These values confirm the suitability of UV-visible spectroscopy for the quantification of NPs in the low μg ml^{-1} range. Calibration data for nanobeads of other sizes are reported in the SI (Fig. S4). The pellets of fragmented PS NPs were resuspended in Milli-Q water, sonicated in a water bath for 20–30 minutes to promote nanoparticle resuspension, and measured using the same protocol adopted for the commercial nanobeads. UV-vis bulk measurements were performed in triplicate in cuvettes with a 1 cm path length (Model V-530, JASCO International Co., Ltd., Tokyo, Japan).

2.4. Pyrolysis-gas chromatography-mass spectrometry

The PS NP suspension was sonicated for 15 minutes and an aliquot of 10 μL was transferred into a pyrolysis cup (PY1-EC80F, 80 μL, Frontier Lab Ltd., Fukushima, Japan) and dried in an oven at 105 °C for 30 minutes. Measurements were performed using an autosampler (AS2020-E, Frontier Lab Ltd., Fukushima, Japan) placed on a microfurnace pyrolyzer (multi-shot pyrolyzer, EGA/Py-3030D, Frontier Lab Ltd., Fukushima, Japan). Once pyrolyzed, the fragments were injected and separated by gas chromatography (7890B, Agilent Technology, Santa Clara, USA, CA), and detected using a single quadrupole

mass spectrometer (5977B MSD, Agilent Technology, Santa Clara, USA, CA).

All samples were analyzed using the single mode of the multi-shot microfurnace and pyrolyzed at 590 °C for 0.3 min, under a helium flow. The pyrolysis fragments were directly injected into the GC column (DB-5MS, 30 m × 0.25 mm × 0.25 μm, Agilent Technology, Santa Clara, USA, CA), with a split ratio of 100 : 1 and a constant helium flow of 1 mL min^{-1}. The GC program started at 40 °C for 2 min and ramped further to 320 °C at a rate of 20 °C min^{-1}, after which the temperature was kept for 14 min. The single quadrupole mass spectrometer was operating in scan mode (*m*/*z* 40–550) at a scan rate of 2.9 scan per second, using electron ionization in positive mode (70 eV). A table summarizing the instrumental parameters is presented in Table S1. The samples were analyzed in triplicate, and empty runs (without cups) were performed to assess any potential cross contamination between samples as well as runs with empty cups to ensure no contamination originating from cup reusage. To overcome any random fluctuations and to ensure comparability between the different samples, 20 μL of a 100 mg L^{-1} poly(4-fluorostyrene), PFS (PSS, Germany), solution in dichloromethane, DCM (CAS 75-09-2, Sigma Aldrich, Germany) was added to each pyrolysis cup as an internal standard. The solvent was evaporated at room temperature before inserting the sample.

The calibration curve was built using a suspension of non-functionalized PS nanobeads with a diameter of 90 nm (Distrilab, The Netherlands). An aqueous suspension of 50 mg L^{-1} of 90 nm PS nanobeads was prepared by diluting the stock solution using MilliQ water (Millipore Co., Burlington, USA, MA). Consequently, five volumes, ranging from 5 to 25 μL, and corresponding to 0.25 to 1.25 μg of PS nanobeads, were transferred into pyrolysis cups, as well as the internal standard, and analyzed with the same method as the samples. The chromatograms were analyzed using the Agilent MassHunter Qualitative Analysis 10.0 Software (Agilent Technologies, Santa Clara, USA, CA), and the styrene trimer was used as a marker compound for the identification (*m*/*z* 312) and quantification (*m*/*z* 91) of the PS NPs.

2.5. Thermogravimetric analysis

Thermogravimetric analysis was performed using a thermogravimetric analyzer (Pyris 1, Perkin Elmer, Shelton, USA, CT). Before the analysis, the PS NP suspension was vortexed for 1 min and sonicated for 30 min in an ultrasonic bath at 25 °C. The entire volume of the NP suspension was used for TGA, since this technique typically requires 1–10 mg of sample. Specifically, 50 μL of the NP suspension was placed in an open platinum pan. The samples were initially heated at 50 °C for 20 minutes under a high-purity nitrogen flow of 20 mL min^{-1} to remove water. Subsequently, the temperature was increased from 50 °C to 600 °C at a heating rate of 10 °C min^{-1}, maintaining the same nitrogen flow. The measurement range was set between 100 and 600 °C, while mass determination was performed in the range of 200–500 °C, as this aligns with the typical degradation range for polymeric and organic materials. Three different samples were analyzed using this procedure. TGA thermograms were analyzed using Pyris™ software.

2.6. Nanoparticle tracking analysis

NTA experiments were performed using a Nanosight NS500Z (Malvern Panalytical, Malvern, UK) instrument equipped with a 405 nm light source. The particle suspensions were diluted 100 times in 0.1 μm filtered MilliQ water and injected in the measurement flow cell by using the peristaltic pump of the instrument. After temperature equilibration at 25 °C and setting the focus, three 60 s long records were acquired (camera level setting of 7) about three different aliquots of each sample by advancing the suspension in the flow cell between measurements. The minimum sample volume used for the analysis was 1 mL. This volume was sufficient to perform five consecutive measurements (pump advancements) without introducing air into the system, as approximately half of the liquid remained in the sample chamber after analysis. Although a single measurement technically requires only 100–200 μL, a total volume of 1 mL is recommended for standard operation, particularly when using manual injection instruments equipped with 1 mL syringes. The collected records were processed using the NTA 3.3 Dev Build 3.3.301 software version applying a detection threshold value of 2 and automatic analysis settings. Three different samples were tested using the same experimental procedure, performing three independent NTA measurements for each sample with three technical replicates, resulting in approximately 4000 valid tracks per sample.

2.7. Atomic force microscopy and nanoplastic size distribution

Pellets of PS NPs were resuspended in Milli-Q water (Millipore Co., Bedford, USA, MA) and briefly sonicated in a water bath for 5 minutes to promote nanoparticle resuspension. An aliquot of 3 μl of the samples were spotted on a freshly cleaved round-shaped mica sheet (grade V-1, thickness 0.1 mm, diameter 10 mm) and air-dried over a heating plate at 37–40 °C (Velp Scientifica, Milan, Italy). Dried samples were then imaged in tapping mode with a JSPM-4210 AFM microscope (JEOL, Japan) equipped with NSC35/ALBS (MikroMasch, Innovative Solutions Bulgaria Ltd., Bulgaria) ultrasharp tips (resonant frequency ≈205 kHz; force constant ≈8.9 N m^{-1}, typical radius tip <10 nm). Topography images were collected over different length scales. To perform a size distribution analysis, AFM images were processed using Gwyddion software. About 10 000 items were counted for size distribution and both the *z*-dimension (height) and the diameter of particles were selected for the analysis.

3. Results & discussion

Independent preparations of fragmented PS NPs were successfully quantified using all the analytical techniques employed: microvolume UV-vis spectroscopy, Py-GC-MS, TGA, and NTA. Subsequently, two independent preparations of PS NPs were simultaneously analyzed using UV-vis spectroscopy and the comparative techniques to evaluate the consistency and comparability of the quantification results.

3.1. Quantification with microvolume UV-visible spectroscopy

UV-vis spectroscopy is a widely used technique for the characterization and quantification of materials and nanomaterials. PS nanobeads present a good absorption in the UV region, with light scattering playing a key role giving rise to some peculiar features appearing thanks to the $\pi \rightarrow \pi^*$ aromatic transitions of the phenyl ring.[30] Testing nanobeads of different sizes, specific nanoparticle characteristics were highlighted. In particular, the wavelength of maximum extinction of PS nanobeads red-shifts (towards longer wavelengths) as the diameter of the nanoparticles increases, as depicted in Fig. 1, due to the contribution of light scattering to the extinction spectrum.[31] PS nanobeads of 100 nm diameter present a sharp peak at around 200 nm, while nanobeads of 1100 nm present a broad extinction band centered around 470 nm. In between, as the nanoparticle diameter increases, the maximum of the extinction peak shifts to longer wavelengths; the position of the maximum is around 240 nm for nanobeads of 300 nm diameter, around 310 nm for nanobeads of 600 nm, and around 390 nm for nanobeads of 800 nm.[32] Parallel to the shift toward higher wavelengths, a reduction in the extinction value is observed (in Fig. 1, all spectra have been normalized to a maximum extinction value of 1 for easier comparison, while Fig. S1 shows the data without normalization). As a result, the need arises for the development of size-specific calibration curves for precise quantification of PS nanobeads.

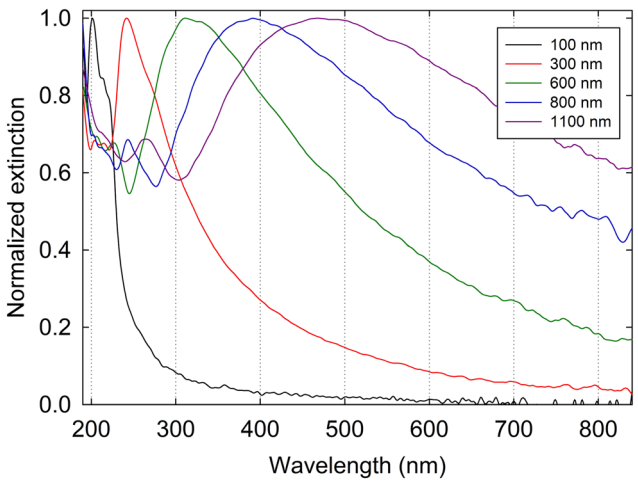

Fig. 1 Normalized UV-vis extinction spectra of polystyrene nanobeads of different diameters at the concentration of 40 μg mL^{-1}.

In order to assess whether spectral differences could be related to phenomena such as nanobead aggregation occurring at the liquid–air interface or any concentration effects, UV-vis bulk measurements were also performed in traditional cuvettes with a 1 cm path length. All PS nanobeads spectra were superimposable to the spectra obtained with the microvolume UV-vis spectrophotometer, as shown in Fig. S2. The dependence of the extinction spectrum on the size of the nanoparticles potentially limits the applicability of the UV-vis spectroscopic technique for the quantification of heterogeneous samples such as fragmented test materials and environmental NPs. However, some consideration can be drawn taking into account the size distribution of NP samples. In Fig. 2b, the size distribution of fragmented NPs obtained from AFM analysis, summing up ten thousand NPs, is reported (with representative AFM images with a scan size of 5 μm and 2 μm displayed in Fig. 2a). This analysis clearly indicates the strong predominance of small NPs of few tens of nanometers, both considering the heights and the diameters of particles, accounting for the presence of in-plane aggregates and tip-driven AFM artifacts.[33] The cumulative size distribution, described in the cumulative percentage curve in

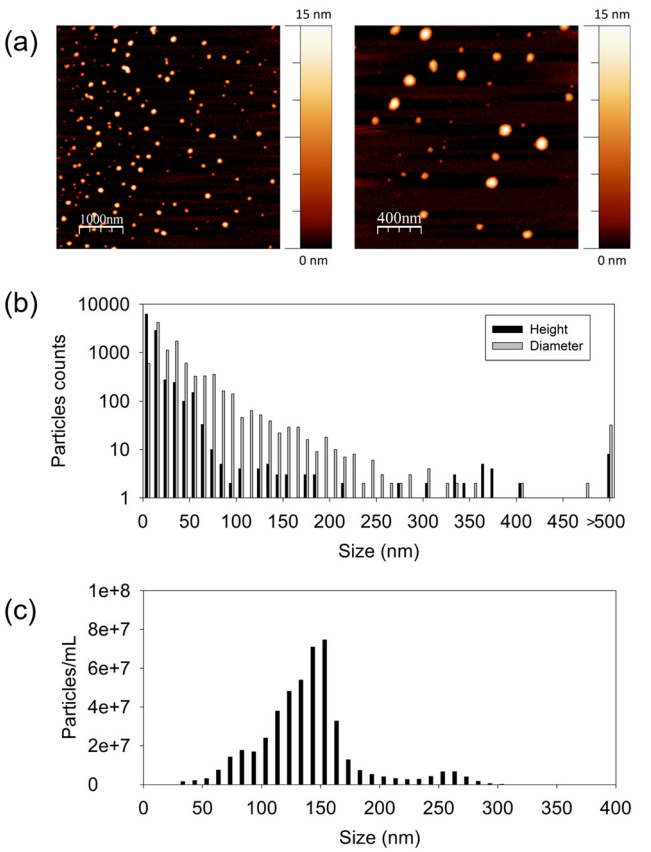

Fig. 2 (a) Atomic force microscopy (AFM) topography images of fragmented polystyrene nanoplastics (scan size of 5 μm and 2 μm), scale bars as indicated (colorimetric scales indicate the maximum height for each image); (b) size distribution of fragmented polystyrene nanoplastics obtained from AFM images. The *y*-axis is on a logarithmic scale; (c) size distribution of fragmented polystyrene nanoplastics obtained with NTA.

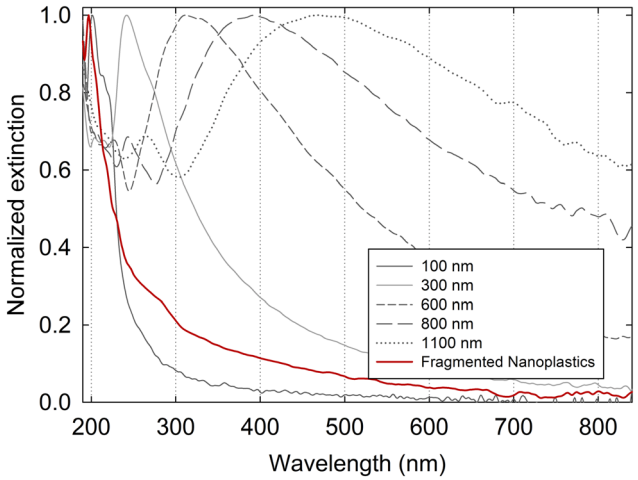

Fig. 3 An example of the UV-vis extinction spectrum of fragmented polystyrene nanoplastics (red curve), in comparison with the spectra of polystyrene nanobeads of increasing size (gray curves).

Fig. S3a, allows the extraction of characteristic percentile values such as D10, D50, and D90, representing the diameters below which 10%, 50%, and 90% of the particle population are found, respectively (D10 = 5.9 nm, D50 = 16.9 nm, and D90 = 66.6 nm). Size distribution analysis performed with NTA confirms the abundance of small nanoparticles, although the distribution is slightly shifted towards larger values. This discrepancy is due to the different measuring principles of AFM and NTA; AFM measures particle's apparent size that can be influenced by tip artifacts, while NTA measures the hydrodynamic diameter. In NTA, detection of the particles depends on their light scattering efficiency and particles with sizes below one tenth of the wavelength of the illuminating laser light are usually not detected. Moreover, when analyzing heterogeneous samples by NTA, the presence of strongly scattering large particles hampers the detection of small particles. The cumulative NTA distribution in Fig. S3b highlights these differences, with D10 = 84.6 nm, D50 = 135.8 nm, and D90 = 180.2 nm, while an example of NTA size distribution of fragmented NPs is shown in Fig. 2c.

Thanks to the dependence of the PS UV-vis extinction spectrum on the size of nanoparticles, UV-vis spectroscopy could represent a useful and rapid way to determine the diameter of monodisperse preparations, as in the case of nanobeads, and even to verify the general size distribution of heterogeneous NP samples. In this sense, an example of the extinction spectrum of the fragmented NPs is presented in Fig. 3. It is important to note that the slight variations in the spectra of fragmented NPs from sample to sample could be attributed to factors such as the heterogeneity of NP samples, variability among different preparations, and the small tested volume. Nevertheless, the extinction peak is generally located between 196 and 220 nm, similarly to what observed for PS nanobeads of 100 nm diameter. The spectra usually present a wider shape, compared to the spectrum of nanobeads, confirming the polydispersity of the fragmented samples.

Given the proximity of the extinction peak of the fragmented NPs to that of 100 nm PS nanobeads, we constructed a calibration curve using 100 nm PS nanobeads and applied it for the quantification of NPs. This approach is based on the assumption that most particles have a diameter of approximately 100 nm, as supported by the size distribution data obtained through AFM and NTA. While this approximation may introduce a measurement error when the actual particle size deviates from the assumed one, it represents a practical solution for samples with a dominant nanoparticle population near 100 nm.

To construct the calibration curve, seven suspensions of 100 nm PS nanobeads with known concentrations ranging from 5 to 100 μg mL^{-1} were analyzed (Fig. 4a), resulting in excellent linearity (R^2 = 0.9994; see Fig. 4b). Calibration curves for PS nanobeads of other sizes were also developed and are presented in Fig. S4.

To estimate the measurement error introduced by using a calibration curve based on nanoparticles of an incorrect size (*viz.* assessing how accurate a calibration curve derived from particles of one size is when applied to particles of different sizes), we performed the following analysis: for each

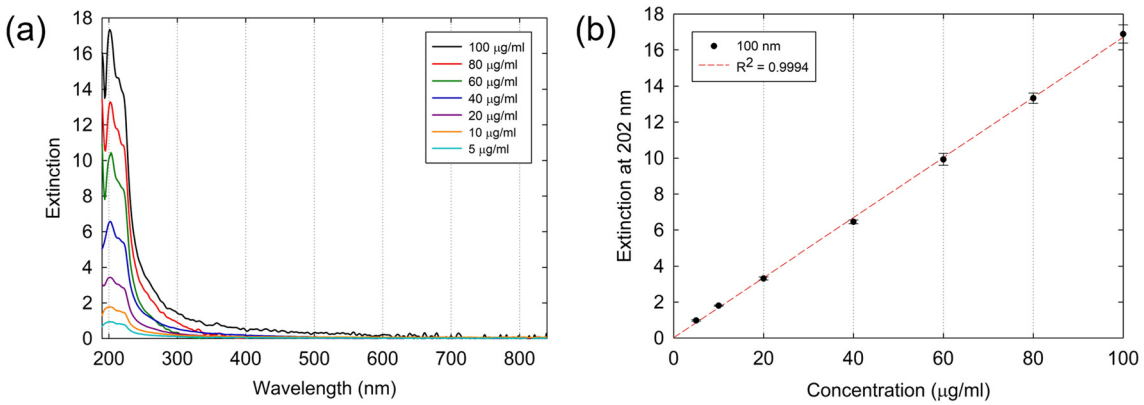

Fig. 4 Calibration curve for 100 nm PS nanobeads. (a) UV-vis spectra; (b) calibration curve. The uncertainty associated with each measurement is expressed as the standard deviation (±SD) of replicate determinations.

nanoparticle size, we interpolated the extinction value corresponding to three different concentrations (40 μg mL^{-1}, 20 μg mL^{-1}, and 10 μg mL^{-1}) using the calibration curves obtained for all other sizes. This allowed us to assess how much the estimated concentration would deviate when using a mismatched calibration curve. For example, a suspension of 100 nm nanoparticles at a true concentration of 20 μg mL^{-1} would be estimated as about 45 μg mL^{-1} if calculated using the calibration curve for 300 nm nanoparticles—more than twice the actual value. Conversely, a suspension of 300 nm nanoparticles at 20 μg mL^{-1} would be estimated as about 9 μg mL^{-1} if using the calibration curve for 100 nm particles—less than half the actual value.

These results, detailed in the SI (Fig. S5), confirm the significant impact of particle size mismatch on quantitative validity and support the conclusion that size-specific calibration curves are necessary to minimize measurement deviations in NP quantification using UV-vis microspectroscopy. When calibration curves derived from smaller particles are used to quantify larger particles, the concentrations are markedly underestimated, while the opposite trend—strongly overestimated—occurs when larger-particle calibrations are applied to smaller ones. This systematic bias is evident across all tested concentrations and becomes particularly critical at lower nominal values, where even small absolute deviations translate into substantial relative errors. The consistent pattern underscores the necessity of particle size-matched calibration for reliable and reproducible quantification.

With the UV-vis analysis, seven independent NP samples have been quantified, performing three replicates for each sample. The measured concentrations ranged from 8.14 ± 0.10 μg mL^{-1} to 26.09 ± 0.19 μg mL^{-1}, corresponding to an equivalent total NP mass ranging from 0.468 ± 0.006 μg to 1.30 ± 0.01 μg in the total sample volumes.

3.2. Quantification with Py-GC-MS

To ensure comparability between UV-vis and Py-GC-MS, the 100 nm PS suspension used for UV-vis quantification was also analyzed by Py-GC-MS, with an estimated concentration of 20 μg mL^{-1}. The concentration obtained using Py-GC-MS was 22.2 ± 3.3 μg mL^{-1}, confirming the reliability of the quantification method. An example of the pyrogram of the fragmented NPs is presented in Fig. 5, analyzed according to the parameters presented in section 2.4. Py-GC-MS presents the great advantage of providing the chemical identification of polymer and the quantification of NPs at once, with a limit of quantification for PS in the nanograms range. On the other hand, the destructive nature of the analysis excludes the recovery of samples for further analysis.

During the pyrolysis process, the PS NPs are fragmented into different pyrolyzates, including styrene (5.165 min), styrene dimer (11.431 min), and styrene trimer (14.893 min). The PFS is fragmented similarly as PS during the pyrolysis, producing three main fragments, including fluorostyrene (5.235 min), fluorostyrene dimer (co-eluting with the styrene dimer) and fluorostyrene trimer (14.783 min).

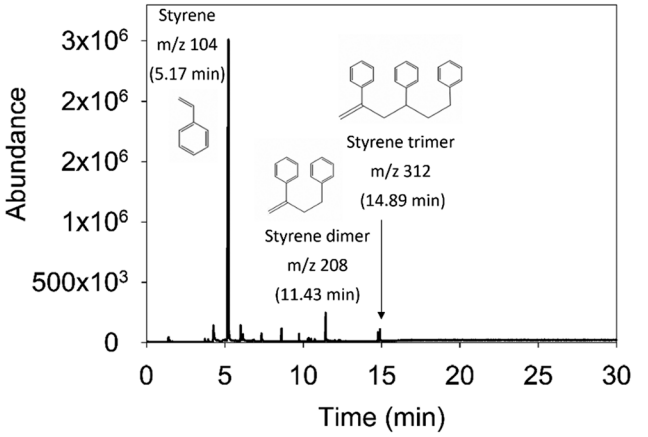

Fig. 5 Total ion chromatogram of polystyrene nanoplastics using poly(4-fluorostyrene) as an internal standard. Major degradation products include styrene (5.165 min), styrene dimer (11.431 min), and styrene trimer (14.893 min) for polystyrene and fluorostyrene (5.235 min), fluorostyrene dimer (co-eluting with the styrene dimer) and fluorostyrene trimer (14.783 min) for poly(4-fluorostyrene).

PS NPs were quantified based on a calibration curve built using 90 nm diameter PS nanobeads, as described in section 2.4 and presented in Fig. S6. The area of the styrene trimer marker (*m*/*z* 91) was extracted from the ion chromatogram of each sample and divided by the extracted area of the fluorostyrene trimer marker (*m*/*z* 109). The choice of the particle diameter size used for the calibration curve is made accordingly to the UV-vis analysis and the laboratory availabilities.

A total of five independent NP samples were analyzed by Py-GC-MS, with two to three technical replicates for each sample. Measured concentrations ranged from 50.1 ± 9.3 μg mL^{-1} to 240 ± 220 μg mL^{-1} corresponding to an equivalent total NP mass ranging from 2.51 ± 0.47 μg to 12.06 ± 11.12 μg in the total samples volumes. Some samples showed a significant standard deviation, indicating inhomogeneity, which could be mitigated by extending the sonication time.

3.3. Quantification with TGA

The TGA thermogram of starting macro PS, used to realize NPs, is presented in Fig. 6a while the TGA of the obtained PS NPs is presented in Fig. 6b.

PS thermal degradation occurs at nearly 400 °C with a single degradation step due to chain breaking, followed by depolymerization with the formation of the styrene monomers, dimers and trimers.[34] The thermal degradation profiles of macro PS and the fragmented PS NPs were notably different, as shown in Fig. 6. The PS NPs exhibited an initial degradation temperature of 196 °C, calculated as the temperature at which 5% weight loss occurred, averaged over the three measurements. This value was significantly lower than the initial degradation temperature of the corresponding pristine

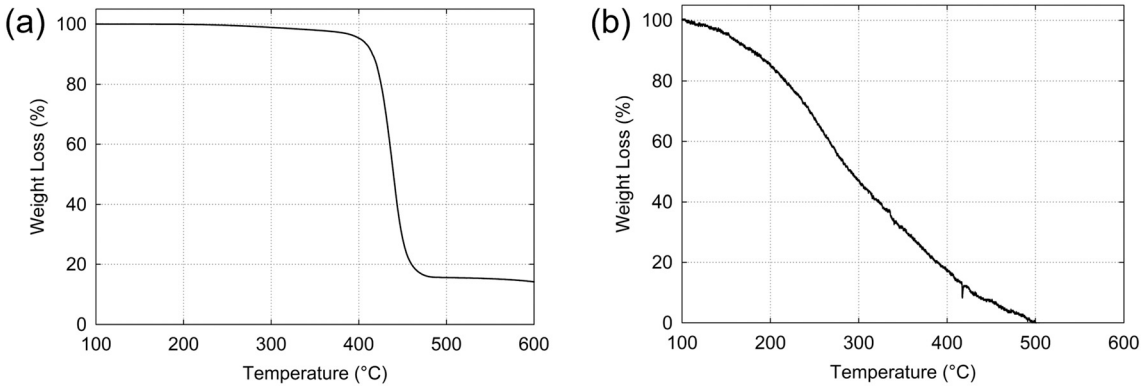

Fig. 6 TGA thermograms of (a) macro polystyrene before fragmentation and (b) fragmented polystyrene nanoplastics.

PS, which was 395 °C. Similar shifts in degradation profiles for NPs were previously reported for polyethylene terephthalate and polyamide NPs, suggesting that degradation of polymers can occur during the mechanical fragmentation process.[17] Variations in thermal behavior of NPs have been widely reported and are often attributed to differences in preparation methods. Specifically, thermal fragmentation of PS has been shown to induce pyrolytic degradation with chain scission, resulting in monomeric units.[35] Likewise, PS nanoparticles prepared *via* microemulsion methods exhibit an onset degradation temperature of 261 °C, which is lower than that of pristine PS.[36]

Shojaeiarani *et al.* (2019) also reported a slight decrease in thermal stability due to polymer degradation occurring during grinding.[37] Furthermore, for polypropylene and polyvinylchloride NPs, smaller particles were found to degrade more rapidly and completely due to their higher surface-to-volume ratios. A reduced residual weight in smaller particles was attributed to the release of inorganic additives during grinding process.[38]

The broader thermal profile observed for PS NPs in this study may result from the combination of different causes such as degradation processes occurring during NP preparation, the lower quantity of material and the smaller particle size. These factors could lead to an earlier degradation onset and a broadening of the degradation steps. The amount of PS NPs was determined calculating the weight loss in the range 200–500 °C. Using TGA, four independent samples were quantified, with results showing that the amount of PS NPs ranged from 0.5 μg to 16 μg per sample. Each measurement was performed on separate independent samples, using the entire available volume, which prevented the possibility of technical replicates.

3.4. Quantification with NTA

An example of the NTA analysis of PS NPs is presented in Fig. 7. NTA is one of the most used light scattering based techniques for the number-based concentration quantification in suspensions of NPs and nanomaterials in general.[39] The great advantage of this analysis is the simultaneous determination of the size-distribution and the number-based concentration of nanoparticles. On the other hand, as with the UV-vis approach, this analysis does not provide any information about the chemical composition of the samples, so it is unable to distinguish between NPs and possible contaminants. The instrument performs well in the 10^8–10^9 particle per mL concentration range in concentration estimation and has a much better resolution in size characterization than batch mode dynamic light scattering (DLS) measurements.[40]

With NTA, three independent NP samples have been quantified, performing three independent NTA measurements for each sample with three technical replicates (for a total of 9 measurements for each sample). The resulting size distributions are known to be affected by the dependence of scattered light intensity from particle diameter and might overestimate the contribution of bigger (more efficient scatterer) particles.[40] NTA results suggest a predominance of small NPs, with mean diameter values ranging from 138.4 ± 8.6 nm to 165.5 ± 11.2 nm. The measured concentrations ranged from $1.70 \times 10^8 \pm 1.82 \times 10^7$ NPs per mL to $5.89 \times 10^8 \pm 3.86 \times 10^7$ NPs per mL.

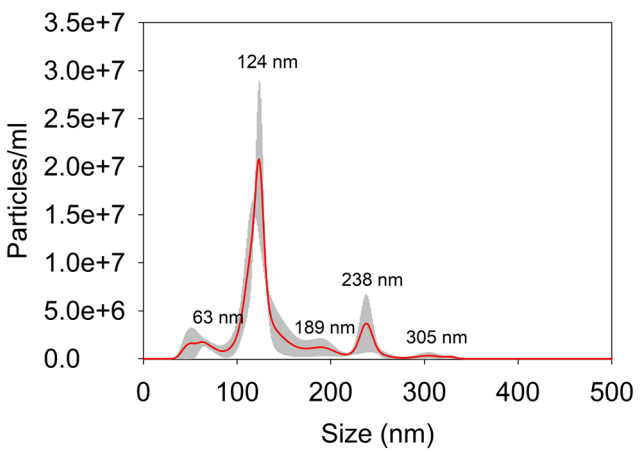

Fig. 7 Example of number-based size distribution of a fragmented polystyrene nanoplastic sample measured by NTA. Red: average of three acquisitions, gray: ± one standard error of the mean.

3.5. Comparing the performance of the different analytical approaches

In this study, a set of analytical techniques were employed to evaluate NP quantification, including microvolume UV-vis spectroscopy, Py-GC-MS, TGA, and NTA. Each of these methods offers unique strengths and limitations, which were carefully considered to provide a comprehensive understanding of the NP content in samples realized through mechanical fragmentation as a top-down approach to realize test materials (Table 1). UV-vis spectroscopy is based on the absorption of ultraviolet and visible light by particles in suspension. The absorption spectrum is related to the particle's size, concentration, and chemical composition. This technique is widely used for its non-destructive nature, rapid analysis, and ease of implementation. However, it is sensitive to interference from sample matrix effects and size-dependent shifts in absorption, which may complicate quantification of heterogeneous samples like fragmented NPs. Py-GC-MS is a thermal decomposition technique that involves heating the sample to high temperatures under an inert atmosphere, breaking it down into smaller, volatile compounds that can be analyzed by gas chromatography coupled with mass spectrometry. This technique provides detailed chemical fingerprints, allowing for the identification and quantification of nanograms to a few micrograms of polymeric material in complex samples. However, Py-GC-MS is destructive and does not provide information on toxicologically relevant parameters such as size and shape, which are critical for understanding the environmental and health risks of NPs. TGA measures the change in mass of a sample as it is heated, providing information on the thermal stability and composition of the sample. This method is particularly useful for quantifying the amount of polymer present in a sample, especially when other components, such as inorganic fillers or additives, are present. One limitation of TGA is its reliance on the complete thermal decomposition of the material, which may not be fully applicable to certain NP types or mixtures. NTA utilizes laser light scattering and Brownian motion to track the movement of nanoparticles in suspension, from which their size distribution and concentration can be determined. NTA is advantageous for its ability to measure particles in real time and its capability to quantify particles in a wide size range. However, it may be affected by sample aggregation and relies on the assumption that particles are spherical and dispersed in a liquid medium.

In the following sections, we will compare the performance of the different proposed techniques, focusing on two main categories: mass-based and number-based methods. The distinction between these approaches is crucial, as they provide different types of data. Mass-based techniques quantify the total mass of NPs in a sample, which is influenced by particle size and density. This method is useful for understanding the overall polymer content but may overestimate the contribution of larger particles and overlook smaller ones, which could be more toxicologically relevant. In contrast, number-based techniques focus on the count, size, and size distribution of particles, offering a more detailed insight into the abundance and dimensions of NPs. Size and shape are particularly important in toxicology, as smaller particles with larger surface areas may present higher reactivity and bioavailability, potentially leading to increased toxicity.

3.5.1. Comparison between mass-based quantification techniques. Mass-based quantification approaches, providing the mass of NPs in a defined volume of suspension (for liquid samples), are the preferred choice in the literature to

Table 1 Comparative overview of the analytical techniques used for true-to-life NP quantification. Note: sample volume refers to the minimum usable volume per replicate. For UV-vis, volume may be recovered; for Py-GC-MS and TGA, the sample is fully consumed

Technique	Type of data	Sample amount required	Sample destruction	Key strengths	Main limitations
Microvolume UV-vis spectroscopy	Mass/number (estimated)	Low (1–2 μL)	No	Rapid and accessible	Underestimates mass in polydisperse samples
				Non-destructive	Requires size-specific calibration
				Minimal sample needed	Affected by scattering and matrix effects
				Useful for trend analysis	
Pyrolysis-GC-MS (Py-GC-MS)	Mass	Moderate (μg scale)	Yes	Chemical identification/ quantification	Destructive
				Suitable for complex matrices	No info on size or shape
Thermogravimetric Analysis (TGA)	Mass	Moderate/high (μg scale)	Yes	Accurate polymer mass quantification	Destructive
				Simple setup	No info on particle size or shape
					Requires larger sample amount
Nanoparticle Tracking Analysis (NTA)	Number	Moderate (mL scale, diluted)	Instrument dependent	Measures size distribution and particle concentration	No info on chemical composition
				Fast	Underestimates small particles
				Widely used in the nanomaterial field	Sensitive to aggregates and optical properties

express the concentration of NPs, since this information is also easily transferable in the context of toxicological and ecotoxicological studies. This is also the common way to report the environmental abundance of environmental pollutants, including NPs.[27]

We selected microvolume UV-vis spectroscopy as a widely available and easy method to quantify realistic NP samples, taking advantage of the low volume sample system, allowing the measurement of scarce samples and the recovery of sample drops after the measurement. This allows saving of samples for subsequent analysis and even for comparison with other quantification techniques, as we performed in this work. The main limitation of this approach was the use of 100 nm PS nanobeads to build the calibration curve, since a sample of realistic NPs produced by mechanical fragmentation, like a sample of real NPs from the environment, is extremely heterogeneous in size and potentially covers the entire nanometer range. Although the choice of using 100 nm nanobeads for the extinction measurement was supported by the size distribution analysis of our NP samples, we acknowledged the need to validate this method by comparing the results with two additional mass-based techniques.

The same two NP samples were quantified using both UV-vis spectroscopy and Py-GC-MS, with the results compared and summarized in Table 2 (samples A and B). The concentration values obtained from UV-vis spectroscopy were generally 3 to 5 times lower than those calculated by Py-GC-MS. This discrepancy can be attributed to the different operating principles of the two methods: UV-vis spectroscopy primarily detects small NPs, while Py-GC-MS analyzes the entire sample, including larger particles and aggregates. As previously mentioned, no size information is provided through Py-GC-MS, and the measured mass reflects the total PS content, including NPs of hundreds of nanometers and aggregates. Considering that a nanoparticle of 100 nm has a mass one thousand times smaller than a 1000 nm nanoparticle, the presence of a few larger nanoparticles significantly influences the total mass measurement, even in samples dominated by smaller NPs.

Three NP samples were quantified with both UV-vis spectroscopy and a third mass-based method, TGA. As reported in Table 2, the amount of NPs measured with TGA for the two samples C and D resulted in approximately one order of magnitude more than the amount calculated with UV-vis spectroscopy. This discrepancy can be attributed to the fact that TGA measures the total mass of the sample, including large nanoparticles and aggregates, whereas UV-vis spectroscopy is more sensitive to smaller particles, as already described for the comparison with Py-GC-MS measurement results. However, we can highlight that the third sample (E, in Table 2) yielded comparable results with both UV-vis and TGA, which may be due to a different degree of heterogeneity in size distribution, where the sample's nanoparticle population might be more homogeneous or predominantly composed of particles in the size range detectable by both methods.

Table 2 Comparison of the total mass (μg) of nanoplastics in each sample, calculated with different mass-based quantification methods

Sample	Microvolume UV-vis	Py-GC-MS	TGA
A	1.305 ± 0.010 μg	4.485 ± 0.003 μg	
B	0.468 ± 0.006 μg	2.51 ± 0.27 μg	
C	0.656 ± 0.009 μg		8.864 μg
D	0.997 ± 0.029 μg		13.432 μg
E	0.362 ± 0.001 μg		0.522 μg

Table 3 Comparison of the total number of nanoplastics in each sample, calculated with UV-vis spectroscopy and NTA

Sample	Microvolume UV-vis	NTA
F	$1.6 \times 10^9 \pm 6.6 \times 10^6$ NPs	$4.2 \times 10^9 \pm 5.4 \times 10^8$ NPs
G	$1.8 \times 10^9 \pm 2.3 \times 10^7$ NPs	$5.9 \times 10^9 \pm 6.3 \times 10^8$ NPs

3.5.2. Comparison with a number-based quantification technique. A second comparison was made between UV-vis spectroscopy and NTA, as a number-based quantification technique. Given the inhomogeneous size distribution of NP samples, skewed towards small nanoparticles, comparing the number of particles rather than their mass may provide a more accurate assessment. To align data derived from UV-vis spectroscopy with those obtained from NTA analysis, we estimated the number of NPs using the PS density (1.05 g cm^{-3}) and a 100 nm particle diameter, which was also used to determine the mass concentration. Two samples were analyzed with both UV-vis spectroscopy and NTA, resulting in comparable concentrations (same order of magnitude) for both samples, as reported in Table 3. As with mass-based techniques, UV-vis spectroscopy generally underestimated the number of NPs compared to NTA, as expected, because large particles and aggregates are not included in the counts.

4. Conclusion

This study demonstrates the applicability of microvolume UV-vis spectroscopy as a rapid, accessible, and non-destructive technique for the quantification of true-to-life PS NPs. While UV-vis spectroscopy offers a rapid and reproducible approach for quantifying NPs, its potential for polymer identification remains limited. Although some polymers may exhibit characteristic absorption bands in the deep UV region, such as $\pi \rightarrow \pi^*$ or $n \rightarrow \pi^*$ transitions associated with specific functional groups, these features are often subtle and may be obscured by the strong scattering contribution in polydisperse or fragmented samples. As a result, the extinction spectra of different polymer types may appear similar under realistic test conditions, especially when particle size and morphology vary. Further investigation is needed to determine whether polymer-specific spectral differences can be reliably resolved, particularly under controlled conditions with minimized scattering. We highlight that future work could explore whether combining UV-vis data with supplementary techniques, such as infrared spectroscopy, Raman, fluorescence emission, or scattering models, may improve polymer discrimination. In this study, UV-vis

spectroscopy is therefore applied exclusively for the quantification of PS-based NPs. The comparison with other well-established mass-based techniques, such as Py-GC-MS and TGA, as well as NTA, a number-based technique, showed good agreement, with the order of magnitude of the measured NP concentrations remaining consistent. This suggests that, despite methodological differences, the overall trends in NP quantification align well across different analytical approaches, reinforcing the reliability of the measurement results and highlighting the value of employing a multitechnique approach for robust and comprehensive NP analysis. UV-vis spectroscopy tends to slightly underestimate NP concentrations compared to mass-based techniques, due to the size-dependent extinction properties of NPs. Nevertheless, UV-vis spectroscopy provides a valuable tool for initial screening and relative quantification of NPs. Its widespread availability, ease of use, and minimal sample consumption make UV-vis spectroscopy a promising candidate for routine NP analysis, especially in toxicological studies where sample quantity is often a limiting factor. Furthermore, while this study focused on PS NPs, the principles demonstrated here suggest that UV-vis spectroscopy could be extended to the quantification of NPs from other polymer types. The feasibility of this approach depends on the polymer's specific optical properties, particularly its absorbance characteristics in the UV-visible range, and the availability of standard nanobeads for building polymer-specific calibration curves. Such an extension would enhance the versatility of UV-vis spectroscopy as a universal tool for NP quantification. Future research directions may also include its coupling with preliminary separation techniques, such as field-flow fractionation, to enhance resolution and selectivity. Further studies should focus on optimizing this method for broader applications and investigating its potential for detecting and quantifying diverse polymeric NPs in environmental and biological matrices.

Author contributions

Serena Ducoli: conceptualization, investigation, methodology, writing – original draft, writing – review & editing. Géraldine Dumont: investigation, methodology, writing – review & editing. Milica Velimirovic: methodology, writing – review & editing. Dora Mehn: investigation, methodology, writing – review & editing. Mariacristina Cocca: investigation, methodology, writing – review & editing. Laura E. Depero: conceptualization, funding acquisition. Stefania Federici: conceptualization, writing – original draft, writing – review & editing.

Conflicts of interest

The authors declare no competing financial interest.

Data availability

Supplementary information is available. See DOI: **https://doi.org/10.1039/D5EN00502G**.

The data within this study is included in either the main article or supplementary information (SI) figures.

Acknowledgements

This article is based upon work from COST Action PRIORITY, CA20101, supported by COST (European Cooperation in Science and Technology). M. V. acknowledges EU-funded project MS4Plastics (H2020-MSCA-IF-2020—Grant Agreement No. 101023205). M. C. and S. F. acknowledge PRIN 2022 Italian project PLASTACTS, Assessment of nano/microplastics impacts (No. 202293AX2L, CUP D53D23009050001). S. D., L. E. D, and S. F. acknowledge with gratitude the support of Prof. Paolo Bergese and his group at the Department of Molecular and Translational Medicine, University of Brescia (Italy) for granting access to the microvolume UV-vis spectrophotometer used in the preliminary measurements.

References

1 S. Allen, D. Allen, S. Karbalaei, V. Maselli and T. R. Walker, Micro(nano)plastics sources, fate, and effects: What we know after ten years of research, *J. Hazard. Mater. Adv.*, 2022, **6**, 100057.
2 W. Fu, J. Min, W. Jiang, Y. Li and W. Zhang, Separation, characterization and identification of microplastics and nanoplastics in the environment, *Sci. Total Environ.*, 2020, **721**, 137561.
3 A. Khan and Z. Jia, Recent insights into uptake, toxicity, and molecular targets of microplastics and nanoplastics relevant to human health impacts, *iScience*, 2023, **26**, 106061.
4 P. K. Rose, S. Yadav, N. Kataria and K. S. Khoo, Microplastics and nanoplastics in the terrestrial food chain: Uptake, translocation, trophic transfer, ecotoxicology, and human health risk, *TrAC, Trends Anal. Chem.*, 2023, **167**, 117249.
5 A. A. Horton and S. J. Dixon, Microplastics: An introduction to environmental transport processes, *Wiley Interdiscip. Rev.: Water*, 2018, **5**, e1268.
6 C. Schwaferts, R. Niessner, M. Elsner and N. P. Ivleva, Methods for the analysis of submicrometer- and nanoplastic particles in the environment, *TrAC, Trends Anal. Chem.*, 2019, **112**, 52–65.
7 J. Gigault, A. ter Halle, M. Baudrimont, P. Y. Pascal, F. Gauffre, T. L. Phi, H. El Hadri, B. Grassl and S. Reynaud, Current opinion: What is a nanoplastic?, *Environ. Pollut.*, 2018, **235**, 1030–1034.
8 S. Reynaud, A. Aynard, B. Grassl and J. Gigault, Nanoplastics: From model materials to colloidal fate, *Curr. Opin. Colloid Interface Sci.*, 2022, **57**, 101528.
9 B. Rani-Borges and R. A. Ando, How small a nanoplastic can be? A discussion on the size of this ubiquitous pollutant, *Cambridge Prisms: Plastics*, 2024, **2**, e23.
10 J. Gigault, H. El Hadri, B. Nguyen, B. Grassl, L. Rowenczyk, N. Tufenkji, S. Feng and M. Wiesner, Nanoplastics are neither microplastics nor engineered nanoparticles, *Nat. Nanotechnol.*, 2021, **16**, 501–507.

11 A. I. Catarino, D. Patsiou, S. Summers, G. Everaert, T. B. Henry and T. Gutierrez, Challenges and recommendations in experimentation and risk assessment of nanoplastics in aquatic organisms, *TrAC, Trends Anal. Chem.*, 2023, **167**, 117262.
12 S. M. Usmani, S. Bremer-Hoffmann, K. Cheyns, F. Cubadda, V. I. Dumit, S. E. Escher, V. Fessard, A. C. Gutleb, T. Léger, Y.-C. Liu, J. Mast, E. McVey, B. Mertens, D. Montalvo, A. G. Oomen, V. Ritz, T. Serchi, H. Sieg, K. Siewert, D. Stanco, E. Verleysen, O. Vincentini, C. W. S. Yeo, D. Yu, M. van der Zande and A. Haase, Review of New Approach Methodologies for Application in Risk Assessment of Nanoparticles in the Food and Feed Sector: Status and Challenges, *EFSA Supporting Publ.*, 2024, **21**, 8826E.
13 F. Blancho, M. Davranche, H. El Hadri, B. Grassl and J. Gigault, Nanoplastics Identification in Complex Environmental Matrices: Strategies for Polystyrene and Polypropylene, *Environ. Sci. Technol.*, 2021, **55**, 8753–8759.
14 D. Materić, R. Holzinger and H. Niemann, Nanoplastics and ultrafine microplastic in the Dutch Wadden Sea – The hidden plastics debris?, *Sci. Total Environ.*, 2022, **846**, 157371.
15 M. Helal, N. B. Hartmann, F. R. Khan and E. G. Xu, Time to integrate "One Health Approach" into nanoplastic research, *Eco-Environ. Health*, 2023, **2**, 18–20.
16 S. Ducoli, G. Kalčíková, M. Velimirovic, L. E. Depero and S. Federici, Production, characterization, and toxicology of environmentally relevant nanoplastics: a review, *Environ. Chem. Lett.*, 2025, **23**, 649–675.
17 S. Ducoli, S. Federici, M. Cocca, G. Gentile, A. Zendrini, P. Bergese and L. E. Depero, Characterization of polyethylene terephthalate (PET) and polyamide (PA) true-to-life nanoplastics and their biological interactions, *Environ. Pollut.*, 2024, **343**, 123150.
18 B. Annangi, A. Villacorta, L. Vela, A. Tavakolpournegari, R. Marcos and A. Hernández, Effects of true-to-life PET nanoplastics using primary human nasal epithelial cells, *Environ. Toxicol. Pharmacol.*, 2023, **100**, 104140.
19 M. J. Huber, N. P. Ivleva, A. M. Booth, I. Beer, I. Bianchi, R. Drexel, O. Geiss, D. Mehn, F. Meier, A. Molska, J. Parot, L. Sørensen, G. Vella, A. Prina-Mello, R. Vogel and F. Caputo, Physicochemical characterization and quantification of nanoplastics: applicability, limitations and complementarity of batch and fractionation methods, *Anal. Bioanal. Chem.*, 2023, **415**, 3007–3031.
20 N. P. Ivleva, S. Primpke and J. M. Lynch, Advances in chemical analysis of micro- and nanoplastics, *Anal. Bioanal. Chem.*, 2023, **415**, 2869–2871.
21 S. Chakraborty, R. Drexel, P. Bhadane, N. Langford, P. Dhumal, F. Meier and I. Lynch, An integrated multimethod approach for size-specific assessment of potentially toxic element adsorption onto micro- and nanoplastics: implications for environmental risk, *Nanoscale*, 2025, **17**, 9122–9136.
22 C. Trujillo, J. Pérez-Arantegui, R. Lobinski and F. Laborda, Improving the Detectability of Microplastics in River Waters by Single Particle Inductively Coupled Plasma Mass Spectrometry, *Nanomaterials*, 2023, **13**, 1582.
23 Y. Xu, Q. Ou, X. Wang, F. Hou, P. Li, J. P. van der Hoek and G. Liu, Assessing the Mass Concentration of Microplastics and Nanoplastics in Wastewater Treatment Plants by Pyrolysis Gas Chromatography-Mass Spectrometry, *Environ. Sci. Technol.*, 2023, **57**, 3114–3123.
24 A. F. Astner, D. G. Hayes, H. O'Neill, B. R. Evans, S. V. Pingali, V. S. Urban, S. M. Schaeffer and T. M. Young, Assessment of cryogenic pretreatment for simulating environmental weathering in the formation of surrogate micro- and nanoplastics from agricultural mulch film, *Sci. Total Environ.*, 2023, **870**, 161867.
25 S. Jung, A. J. Raghavendra and A. K. Patri, Comprehensive analysis of common polymers using hyphenated TGA-FTIR-GC/MS and Raman spectroscopy towards a database for micro- and nanoplastics identification, characterization, and quantitation, *NanoImpact*, 2023, **30**, 100467.
26 Y. Li, Z. Wang and B. Guan, Separation and identification of nanoplastics in tap water, *Environ. Res.*, 2022, **204**, 112134.
27 D. Materić, H. A. Kjær, P. Vallelonga, J. L. Tison, T. Röckmann and R. Holzinger, Nanoplastics measurements in Northern and Southern polar ice, *Environ. Res.*, 2022, **208**, 112741.
28 S. Ducoli, S. Federici, R. Nicsanu, A. Zendrini, C. Marchesi, L. Paolini, A. Radeghieri, P. Bergese and L. E. Depero, A different protein corona cloaks "true-to-life" nanoplastics with respect to synthetic polystyrene nanobeads, *Environ. Sci.: Nano*, 2022, **9**, 1414–1426.
29 The IUPAC Compendium of Chemical Terminology, The IUPAC Compendium of Chemical Terminology, DOI: **10.1351/GOLDBOOK.**
30 M. Andrini, S. Federici and L. Gavioli, Refractive Index of Benchmark Polystyrene Nanoplastics by Optical Modeling of UV-Vis Spectra, *Anal. Chem.*, 2025, **97**, 19419–19426.
31 G. S. He, H. Y. Qin and Q. Zheng, Rayleigh, Mie, and Tyndall scatterings of polystyrene microspheres in water: Wavelength, size, and angle dependences, *J. Appl. Phys.*, 2009, **105**, 023110.
32 X. Wang and Y. Cao, Characterizations of absorption, scattering, and transmission of typical nanoparticles and their suspensions, *J. Ind. Eng. Chem.*, 2020, **82**, 324–332.
33 F. Gołek, P. Mazur, Z. Ryszka and S. Zuber, AFM image artifacts, *Appl. Surf. Sci.*, 2014, **304**, 11–19.
34 A. I. Roland and G. Schmidt-Naake, Thermal degradation of polystyrene produced by nitroxide-controlled radical polymerization, *J. Anal. Appl. Pyrolysis*, 2001, **58–59**, 143–154.
35 Y. K. Song, S. H. Hong, S. Eo and W. J. Shim, The fragmentation of nano- and microplastic particles from thermoplastics accelerated by simulated-sunlight-mediated photooxidation, *Environ. Pollut.*, 2022, **311**, 119847.
36 B. Davodi, M. S. Lashkenari and H. Eisazadeh, Fabrication and thermal degradation behavior of polystyrene nanoparticles coated with smooth polyaniline, *Synth. Met.*, 2011, **161**, 1207–1210.
37 J. Shojaeiarani, D. S. Bajwa, C. Rehovsky, S. G. Bajwa and G. Vahidi, Deterioration in the Physico-Mechanical and Thermal Properties of Biopolymers Due to Reprocessing, *Polymers*, 2019, **11**, 58.

38 L. A. Parker, E. M. Höppener, E. F. van Amelrooij, S. Henke, I. M. Kooter, K. Grigoriadi, M. G. A. Nooijens, A. M. Brunner and A. Boersma, Protocol for the production of micro- and nanoplastic test materials, *Microplast. Nanoplast.*, 2023, **3**, 10.

39 F. Caputo, R. Vogel, J. Savage, G. Vella, A. Law, G. Della Camera, G. Hannon, B. Peacock, D. Mehn, J. Ponti, O. Geiss, D. Aubert, A. Prina-Mello and L. Calzolai, Measuring particle size distribution and mass concentration of nanoplastics and microplastics: addressing some analytical challenges in the sub-micron size range, *J. Colloid Interface Sci.*, 2021, **588**, 401–417.

40 V. Filipe, A. Hawe and W. Jiskoot, Critical Evaluation of Nanoparticle Tracking Analysis (NTA) by NanoSight for the Measurement of Nanoparticles and Protein Aggregates, *Pharm. Res.*, 2010, **27**, 796.